

Faster and more accurate computation of the \mathcal{H}_∞ norm via optimization

Peter Benner* Tim Mitchell†

December 14, 2024

Abstract

In this paper, we propose an improved method for computing the \mathcal{H}_∞ norm of linear dynamical systems that results in a code that is often several times faster than existing methods. Our approach uses standard optimization tools to rebalance the work load of the standard algorithm due to Boyd, Balakrishnan, Bruinsma, and Steinbuch, with the aim of minimizing the number of expensive eigenvalue computations that must be performed. Unlike the standard algorithm, our improved approach can also calculate the \mathcal{H}_∞ norm to full precision with little extra work, and also offers some opportunity to improve its performance via parallelization. Finally, our improved method is also applicable for approximating the \mathcal{H}_∞ norm of large-scale systems.

1 Introduction

Consider the continuous-time linear dynamical system

$$E\dot{x} = Ax + Bu \tag{1a}$$

$$y = Cx + Du, \tag{1b}$$

where $A \in \mathbb{C}^{n \times n}$, $B \in \mathbb{C}^{n \times p}$, $C \in \mathbb{C}^{m \times n}$, $D \in \mathbb{C}^{m \times p}$, and $E \in \mathbb{C}^{n \times n}$. The system defined by (1) arises in many engineering applications and as a consequence, there has been a strong motivation for fast methods to compute properties that measure the sensitivity of the system or its robustness to noise. Specifically, a quantity of great interest is the \mathcal{H}_∞ norm, which is defined as

$$\|G\|_{\mathcal{H}_\infty} := \sup_{\omega \in \mathbb{R}} \|G(\mathbf{i}\omega)\|_2, \tag{2}$$

where

$$G(\lambda) = C(\mathbf{i}\omega E - A)^{-1}B + D \tag{3}$$

*Max Planck Institute for Dynamics of Complex Technical Systems, Magdeburg, 39106 Germany (benner@mpi-magdeburg.mpg.de).

†Max Planck Institute for Dynamics of Complex Technical Systems, Magdeburg, 39106 Germany (mitchell@mpi-magdeburg.mpg.de).

is the associated *transfer function* of the system given by (1). The \mathcal{H}_∞ norm measures the maximum sensitivity of the system; in other words, the higher the value of the \mathcal{H}_∞ norm, the less robust the system is. The \mathcal{H}_∞ norm is also a key metric for assessing the quality of reduced-order models that attempt to capture/mimic the dynamical behavior of large-scale systems, see, e.g., [Ant05, BCOW17].

When $E = I$, (2) is finite as long as A is stable, whereas an unstable system would be considered infinitely sensitive. If $E \neq I$, then (1) is called a *descriptor system*. Assuming that E is singular but (A, E) is regular and at most index 1, then (2) still yields a finite value, provided that all the controllable and observable eigenvalues of (A, E) are finite and in the open left half plane, where for λ an eigenvalue of (A, E) with right and left eigenvectors x and y , λ is considered *uncontrollable* if $B^*y = 0$ and *unobservable* if $Cx = 0$. However, the focus of this paper is not about detecting when (2) is infinite or finite, but to introduce an improved method for computing the \mathcal{H}_∞ norm when it is finite. Thus, for conciseness in presenting our improved method, we will assume in this paper that any system provided to an algorithm has a finite \mathcal{H}_∞ norm, as checking whether it is infinite can be considered a preprocessing step.¹

While the first algorithms [BBK89, BB90, BS90] for computing the \mathcal{H}_∞ norm date back to nearly 30 years ago, there has been continued interest in improved methods, particularly as the state-of-art methods remain quite expensive with respect to their dimension n , meaning that computing the \mathcal{H}_∞ norm is generally only possible for rather small-dimensional systems. In 1998, [GVV98] proposed an interpolation refinement to the existing algorithm of [BB90, BS90] to accelerate its rate of convergence. More recently, in 2011, [BP11] presented an entirely different approach to computing the \mathcal{H}_∞ norm, by finding isolated common zeros of two certain bivariate polynomials. While they showed that their method was much faster than an implementation of [BB90, BS90] on two SISO examples (single-input, single-output, that is, $m = p = 1$), more comprehensive benchmarking does not appear to have been done yet. Shortly thereafter, [BSV12] extended the now standard algorithm of [BB90, BS90] to descriptor systems. There also has been a very recent surge of interest in efficient \mathcal{H}_∞ norm approximation methods for large-scale systems. These methods fall into two broad categories: those that are applicable for descriptor systems with possibly singular E matrices but require solving linear systems [BV14, FSV14, ABM⁺16] and those that don't solve linear systems but require that $E = I$ or that E is at least cheaply inverted [GGO13, MO16]. Our contribution in this paper is applicable to both improving upon the methods of [BB90, BS90, GVV98] for *computing* the \mathcal{H}_∞ norm (to machine precision) and for *approximating* it in large-scale settings.

The paper is organized as follows. In Sections 2 and 3, we describe the standard algorithms for computing the \mathcal{H}_∞ norm and then give an overview of their computational costs. In Section 4, we introduce our new approach to computing the \mathcal{H}_∞ norm via leveraging optimization techniques. Section 5 describes how the results and algorithms are adapted for discrete-time problems. We present numerical results in Section 6 and concluding remarks in Section 7.

¹We note that while our proposed improvements are also directly applicable for computing the \mathcal{L}_∞ norm, we will restrict the discussion here to just the \mathcal{H}_∞ norm for brevity.

2 The standard algorithm for computing the \mathcal{H}_∞ norm

We begin by presenting a key theorem relating the singular values of the transfer function to purely imaginary eigenvalues of an associated matrix pencil. For the case of simple ODEs, where $B = C = E = I$ and $D = 0$, the result goes back to [Bye88, Theorem 1], and was first extended to linear dynamical systems with input and output with $E = I$ in [BBK89, Theorem 1], and then most recently generalized to systems where $E \neq I$ in [BSV12, Theorem 1]. We state the theorem without the proof, since it is readily available in [BSV12].

Theorem 2.1. *Let $\lambda E - A$ be regular with no finite eigenvalues on the imaginary axis, $\gamma > 0$ not a singular value of D , and $\omega \in \mathbb{R}$. Consider the matrix pencil $(\mathcal{M}_\gamma, \mathcal{N})$, where*

$$\mathcal{M}_\gamma := \begin{bmatrix} A - BR^{-1}D^*C & -\gamma BR^{-1}B^* \\ \gamma C^*S^{-1}C & -A^* + C^*DR^{-1}B^* \end{bmatrix} \text{ and } \mathcal{N} := \begin{bmatrix} E & 0 \\ 0 & E^* \end{bmatrix} \quad (4)$$

and $R = D^*D - \gamma^2 I$ and $S = DD^* - \gamma^2 I$. Then $i\omega$ is an eigenvalue of matrix pencil $(\mathcal{M}_\gamma, \mathcal{N})$ if and only if γ is a singular value of $G(i\omega)$.

Theorem 2.1 immediately leads to an algorithm for computing the \mathcal{H}_∞ norm based on computing the imaginary eigenvalues, if any, of the associated matrix pencil (4). For brevity in this section, we assume that $\max \|G(i\omega)\|_2$ is not attained at $\omega = \infty$, in which case the \mathcal{H}_∞ norm would be $\|D\|_2$. Evaluating the norm of the transfer function for any finite frequency along the imaginary axis immediately gives a lower bound to the \mathcal{H}_∞ norm while an upper bound can be obtained by successively increasing γ until the matrix pencil given by (4) no longer has any purely imaginary eigenvalues. Then, it is straightforward to compute the \mathcal{H}_∞ norm using bisection, as first proposed in [BBK89].

As Theorem 2.1 provides a way to calculate all the frequencies where $g_c(\omega) = \gamma$, it was shortly thereafter proposed in [BB90, BS90] that instead of computing an upper bound and then using bisection, the initial lower bound could be successively increased in a monotonic fashion to the value of the \mathcal{H}_∞ norm. For convenience, it will be helpful to establish the following notation for the transfer function and its largest singular value, both as parameters of frequency ω :

$$G_c(\omega) := G(i\omega) \quad (5)$$

$$g_c(\omega) := \|G(i\omega)\|_2 = \|G_c(\omega)\|_2. \quad (6)$$

Let $\{\omega_1, \dots, \omega_l\}$ be the set of imaginary parts of the purely imaginary eigenvalues of (4) for the initial value γ , sorted in increasing order. Considering the intervals $I_k = [\omega_k, \omega_{k+1}]$, [BS90] proposed increasing γ via:

$$\gamma_{\text{mp}} = \max g_c(\hat{\omega}_k) \quad \text{where} \quad \hat{\omega}_k \text{ are the midpoints of the intervals } I_k. \quad (7)$$

Simultaneously and independently, a similar algorithm was proposed by [BB90], with the additional results that (a) it was possible to calculate which intervals I_k satisfied $g_c(\omega) \geq \gamma$ for all $\omega \in I_k$, thus reducing the number of evaluations of $g_c(\omega)$ needed at every iteration, and (b) this midpoint scheme actually had a local quadratic rate of convergence, greatly improving upon the linear rate of convergence of the earlier, bisection-based method. This midpoint-based method, which we refer to as the BBBS algorithm

Algorithm 1 The Standard BBBS Algorithm

Input: $A \in \mathbb{C}^{n \times n}$, $B \in \mathbb{C}^{n \times p}$, $C \in \mathbb{C}^{m \times n}$, $D \in \mathbb{C}^{m \times p}$, $E \in \mathbb{C}^{n \times n}$ and $\omega_0 \in \mathbb{R}$.

Output: $\gamma = \|G\|_{\mathcal{H}_\infty}$ and ω such that $\gamma = g_c(\omega)$.

```

1:  $\gamma = g_c(\omega_0)$ 
2: while not converged do
3:   // Compute the intervals that lie under  $g_c(\omega)$  using eigenvalues of the pencil:
4:   Compute  $\Lambda_I = \{\text{Im } \lambda : \lambda \in \Lambda(\mathcal{M}_\gamma, \mathcal{N}) \text{ and } \text{Re } \lambda = 0\}$ .
5:   Index and sort  $\Lambda_I = \{\omega_1, \dots, \omega_l\}$  s.t.  $\omega_j \leq \omega_{j+1}$ .
6:   Form all intervals  $I_k = [\omega_k, \omega_{k+1}]$  s.t.  $g'_c(\omega_k) \geq 0$  and  $g'_c(\omega_{k+1}) \leq 0$ .
7:   // Compute candidate frequencies for each interval:
8:   Compute midpoints  $\hat{\omega}_k = 0.5(\omega_k + \omega_{k+1})$  for each interval  $I_k$ .
9:   // Update to the highest gain evaluated at these candidate frequencies:
10:   $\omega = \arg \max g_c(\hat{\omega}_k)$ .
11:   $\gamma = g_c(\omega)$ .
12: end while

```

NOTE: The quartically converging variant proposed by [GVV98] replaces the midpoints of I_k with the maximizing frequencies of Hermite cubic interpolants, which are uniquely determined by interpolating the values of $g_c(\omega)$ and $g'_c(\omega)$ at both endpoints of each interval I_k .

for its authors Boyd, Balakrishnan, Bruinsma, and Steinbuch, is now considered the standard algorithm for computing the \mathcal{H}_∞ norm and it is the algorithm implemented in the MATLAB Robust Control Toolbox, e.g. routine `hinfnorm`. Algorithm 1 provides a high-level pseudocode description for the standard BBBS algorithm while Figure 1a provides a corresponding pictorial description of how the method works.

In [GVV98], a refinement to the BBBS algorithm was proposed which increased its local quadratic rate of convergence to quartic. This was done by evaluating $g_c(\omega)$ at the maximizing frequencies of the unique cubic Hermite interpolants for each interval, instead of at the midpoints. That is, for each interval $I_k = [\omega_k, \omega_{k+1}]$, the unique interpolant $c_k(\omega) = c_3\omega^3 + c_2\omega^2 + c_1\omega + c_0$ is constructed so that

$$\begin{aligned} c_k(\omega_k) &= g_c(\omega_k) & c'_k(\omega_k) &= g'_c(\omega_k) \\ c_k(\omega_{k+1}) &= g_c(\omega_{k+1}) & c'_k(\omega_{k+1}) &= g'_c(\omega_{k+1}). \end{aligned} \quad (8)$$

Then, γ is updated via

$$\gamma_{\text{cubic}} = \max g_c(\hat{\omega}_k) \quad \text{where} \quad \hat{\omega}_k = \arg \max_{\omega \in I_k} c_k(\omega), \quad (9)$$

that is, $\hat{\omega}_k$ is now the maximizing value of interpolant $c_k(\omega)$ on its interval I_k , which of course can be cheaply and explicitly computed. In [GVV98], the single numerical example shows the concrete benefit of this interpolation scheme, where the standard BBBS algorithm required six eigenvalue decompositions of (4) to converge, while their new method only required four. As only the selection of the ω_k values is different, the pseudocode for this improved version of the BBBS algorithm remains largely the same,

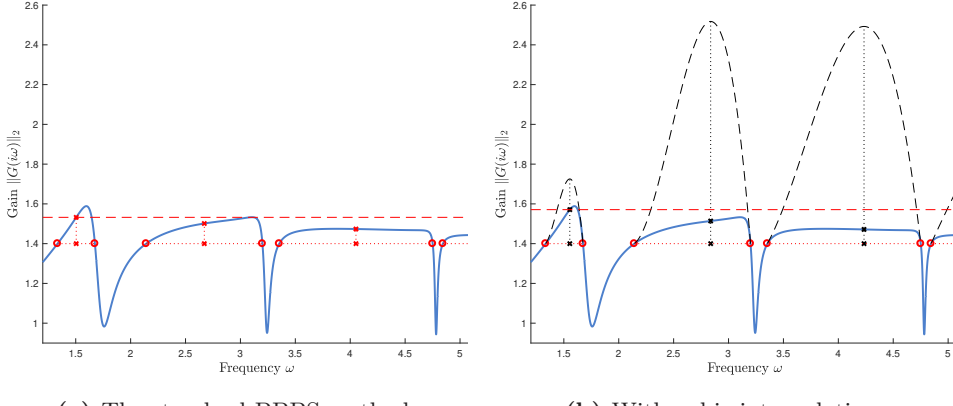


Figure 1: The blue curves show the value of $g_c(\omega) = \|G(\mathbf{i}\omega)\|_2$ while the red circles mark the frequencies $\{\omega_1, \dots, \omega_l\}$ where $g_c(\omega) = \gamma = 1.4$, computed by taking the imaginary parts of the purely imaginary eigenvalues of (4) on a sample problem. The left plot shows the midpoint scheme of the standard BBBS algorithm to obtain an increased value for γ , depicting by the dashed horizontal line. The right plot shows the cubic interpolation refinement of [GVV98] for the same problem and initial value of γ . The dashed black curves depict the cubic Hermite interpolants for each interval while the dotted vertical lines show their respective maximizing frequencies. As can be seen, the cubic interpolation scheme results in a larger increase in γ (again represented by the dashed horizontal line) compared to the standard BBBS method on this iterate for this problem.

as mentioned in the note of Algorithm 1. Figure 1b provides a corresponding pictorial description of the cubic-interpolant-based refinement.

As it turns out, computing the derivatives in (8) for the Hermite interpolations of each interval can also be done with little extra work. Recalling that $g_c(\omega)$ is the largest singular value of $G_c(\omega)$, assume that $g_c(\omega)$ is a simple singular value and that it is smoothly varying in a neighborhood about some value $\hat{\omega} \in \mathbb{R}$, that is, all other singular values of $G_c(\omega)$ are strictly less than $g_c(\omega)$ in this neighborhood. Let $u(\omega)$ and $v(\omega)$ be the associated left and right singular vectors of $g_c(\omega)$. Then, it follows by standard perturbation theory that

$$g'_c(\omega) \Big|_{\omega=\hat{\omega}} = \operatorname{Re} (u(\hat{\omega})^* G'_c(\hat{\omega}) v(\hat{\omega})), \quad (10)$$

where, by standard matrix differentiation rules with respect to parameter ω ,

$$G'_c(\omega) = -\mathbf{i}C(\mathbf{i}\omega E - A)^{-1} E (\mathbf{i}\omega E - A)^{-1} B. \quad (11)$$

As shown in [SVT95], it is actually fairly cheap to compute (10) if the eigenvectors of (4) have also been computed, as there is a correspondence between the eigenvectors of the imaginary eigenvalues of (4) and the associated singular vectors for γ . For $\gamma = g_c(\hat{\omega})$, if $[q^T s^T]^T$ is an eigenvector of (4) for imaginary eigenvalue $\mathbf{i}\hat{\omega}$, then the equivalences

$$q = (\mathbf{i}\hat{\omega} E - A)^{-1} B v(\hat{\omega}) \quad \text{and} \quad s = (\mathbf{i}\hat{\omega} E - A)^{-*} C^* u(\hat{\omega}) \quad (12)$$

both hold, where $u(\hat{\omega})$ and $v(\hat{\omega})$ are left and right singular vectors associated with $g_c(\hat{\omega})$. (To see why these equivalences hold, we refer the reader to the proof of Theorem 5.1 for the discrete-time analog result.) Thus, (10) may be rewritten as follows:

$$g'_c(\omega) \Big|_{\omega=\hat{\omega}} = \operatorname{Re} (u(\hat{\omega})^* G'_c(\hat{\omega}) v(\hat{\omega})) \quad (13)$$

$$= -\operatorname{Re} \left(u(\hat{\omega})^* \mathbf{i}C (\mathbf{i}\hat{\omega}E - A)^{-1} E (\mathbf{i}\hat{\omega}E - A)^{-1} B v(\hat{\omega}) \right) \quad (14)$$

$$= -\operatorname{Re} (\mathbf{i}s^* E q), \quad (15)$$

and it is thus clear that (10) is cheaply computable for all the endpoints of the intervals I_k , provided that the eigenvalue decomposition of (4) has already been computed.

3 The computational costs involved in the BBBS algorithm

The main drawback of the BBBS algorithm is its algorithmic complexity, which is $\mathcal{O}(n^3)$ work per iteration. This not only limits the tractability of computing the \mathcal{H}_∞ norm to rather low-dimensional (in n) systems but can also make computing the \mathcal{H}_∞ norm to full precision an expensive proposition for even moderately-sized systems. In fact, the default tolerance for `hinfnorm` in MATLAB is set quite large, 0.01, presumably to keep its runtime as fast as possible, at the expense of sacrificing accuracy. In Table 1, we report the relative error of computing the \mathcal{H}_∞ norm when using `hinfnorm`'s default tolerance of 0.01 compared to 10^{-14} , along with the respective runtimes for several test problems, observing that computing the \mathcal{H}_∞ norm to near full precision often takes about three times longer. While computing only a handful of the most significant digits of the \mathcal{H}_∞ norm may be sufficient for some applications, this is certainly not true in general. Indeed, the source code for HIFOO [BHLO06], which designs \mathcal{H}_∞ norm fixed-order optimizing controllers for a given open-loop system via nonsmooth optimization, specifically contains the comment regarding `hinfnorm`: “default is .01, which is too crude”. In HIFOO, the \mathcal{H}_∞ norm is minimized by updating the controller variables at every iteration but the optimization method assumes that the objective function is continuous; if the \mathcal{H}_∞ norm is not calculated sufficiently accurately, then it may appear to be discontinuous, which can cause the underlying optimization method to break down. Thus there is motivation to not only improve the overall runtime of computing the \mathcal{H}_∞ norm for large tolerances, but to also to make the computation as fast as possible when computing the \mathcal{H}_∞ norm to full precision.

The dominant cost of the BBBS algorithm is computing the eigenvalues of (4) at every iteration. Even though the method converges quadratically, and quartically when using the cubic interpolation refinement, the eigenvalues of $(\mathcal{M}_\gamma, \mathcal{N})$ will still generally be computed for multiple values of γ before convergence, for either variant of the algorithm. Furthermore, pencil $(\mathcal{M}_\gamma, \mathcal{N})$ is $2n \times 2n$, meaning that the $\mathcal{O}(n^3)$ work per iteration also contains a significant constant factor, specifically eight. If cubic interpolation is used, computing the derivatives (10) via (15) using the eigenvectors of $(\mathcal{M}_\gamma, \mathcal{N})$ requires an additional $4n^2$ doubles (assuming 64-bit computation) worth of memory to store them. This can be a particularly wasteful use of memory during the final iterates

$h = \text{hinfnorm}(\cdot, 1e-14)$ versus $\hat{h} = \text{hinfnorm}(\cdot, 0.01)$							
Problem	Dimensions			$E = I$	$\frac{\hat{h}-h}{h}$	Wall-clock time (sec.)	
	n	p	m			$\text{tol}=1e-14$	$\text{tol}=0.01$
CBM	351	1	2	Y	-4.2×10^{-5}	3.050	2.928
CSE2	63	1	32	Y	-2.5×10^{-4}	0.131	0.093
CM3	123	1	3	Y	-2.7×10^{-3}	0.142	0.055
CM4	243	1	3	Y	-4.7×10^{-3}	1.514	0.708
ISS	270	3	3	Y	-1.0×10^{-6}	0.713	0.455
FOM	1006	1	1	Y	-1.8×10^{-5}	100.774	35.384
NN18	1006	1	2	Y	-1.8×10^{-5}	100.783	35.798
randn 1	500	300	300	Y	0	21.079	24.209
randn 2	600	150	150	N	-6.1×10^{-8}	27.315	15.698

Table 1: For various problems, the relative error of computing \mathcal{H}_∞ norm using `hinfnorm` with its loose default tolerance is shown. Using `hinfnorm` to compute the \mathcal{H}_∞ norm to near machine precision often takes up to nearly three times longer.

of the algorithm, when $(\mathcal{M}_\gamma, \mathcal{N})$ typically will only have a handful of purely imaginary eigenvalues (often just two) and thus only a handful of the $2n$ eigenvectors are actually needed. Finally, computing the purely imaginary eigenvalues of $(\mathcal{M}_\gamma, \mathcal{N})$ using the regular QZ algorithm can be ill advised; in practice, rounding error in the real parts of the eigenvalues can make it difficult to detect which of the computed eigenvalues are supposed to be the purely imaginary ones and which are merely just close to the imaginary axis. Indeed, purely imaginary eigenvalues can easily be perturbed off of the imaginary axis when using standard QZ; [BSV16, Figure 4] illustrates this issue particularly well. Failure to properly identify the purely imaginary eigenvalues can cause the BBBS algorithm to return incorrect results. As such, it is instead recommended [BSV12, Section II.D] to use the specialized Hamiltonian-structure-preserving eigensolvers of [BBMX02, BSV16] to avoid this problem. However, doing so can be even more expensive as it requires computing the eigenvalues of a related matrix pencil that is even larger: $(2n + m + p) \times (2n + m + p)$.

On the other hand, computing (6), the norm of the transfer function, is typically rather inexpensive, at least relative to computing the imaginary eigenvalues of the matrix pencil (4); see Table 2 for data on how much faster computing the singular value decomposition of $G(\mathbf{i}\omega)$ typically is compared to computing the eigenvalues of $(\mathcal{M}_\gamma, \mathcal{N})$ (using regular QZ) for a selection of randomly-generated systems composed of dense matrices of various dimensions. As can be seen, computing the eigenvalues of (4) for tiny systems can take up to two-and-a-half times longer than computing the SVD of $G(\mathbf{i}\omega)$ on modern hardware, while for larger systems where $m, p \ll n$ (the typical case in practice), this performance gap dramatically widens to about 120 times longer. Of course, this disparity in runtime speeds is not entirely surprising. Computing the eigenvalues of (4) involves working with a $2n \times 2n$ (or larger when using structure-preserving eigensolvers) matrix pencil while the main costs to evaluate the norm of the transfer function at a particular frequency involve first solving a linear system of dimension n to

Computing $\ G(\mathbf{i}\omega)\ _2$ versus $\text{eig}(\mathcal{M}_\gamma, \mathcal{N})$					
			Times faster		
n	m	p	min	max	
20	20	20	0.71	2.47	
100	100	100	6.34	10.2	
400	400	400	19.2	36.8	
400	10	10	78.5	119.0	

Table 2: The range of how many times faster computing $\|G(\mathbf{i}\omega)\|_2$ is compared to $\text{eig}(\mathcal{M}_\gamma, \mathcal{N})$ for five trials of randomly generated dense systems of various dimensions.

compute either the $(\mathbf{i}\omega E - A)^{-1}B$ or $C(\mathbf{i}\omega E - A)^{-1}$ term in $G(\mathbf{i}\omega)$ and then computing the maximum singular value of $G(\mathbf{i}\omega)$, which is $m \times p$. If $\min(m, p)$ is small, the cost to compute the largest singular value is negligible and even if $\min(m, p)$ is not small, the largest singular value can still typically be computed easily and efficiently using sparse methods. Solving the n -dimensional linear system is typically going to be much cheaper than computing the eigenvalues of the $2n \times 2n$ pencil, and more so if A and E are not dense and $(\mathbf{i}\omega E - A)$ permits fast (sparse) LU decomposition.

4 The improved algorithm

Recall that computing the \mathcal{H}_∞ norm is done by maximizing $g_c(\omega)$ over $\omega \in \mathbb{R}$ but that the BBBS algorithm (and the cubic interpolation refinement) actually converges to a global maximum of $g_c(\omega)$ by iteratively computing the eigenvalues of the large matrix pencil $(\mathcal{M}_\gamma, \mathcal{N})$ for successively larger values of γ . However, we could alternatively consider a more direct approach of finding maximizers of $g_c(\omega)$, which as discussed above, is a much cheaper function to evaluate numerically. Doing so would hopefully minimize the number of times that the eigenvalues of $(\mathcal{M}_\gamma, \mathcal{N})$ must be computed, and thus speed up the running time of the algorithm.

Though $g_c(\omega)$ is typically nonconvex, standard optimization methods should generally still be able to find local maximizers, if not always global maximizers, provided that $g_c(\omega)$ is sufficiently smooth. Since $g_c(\omega)$ is the maximum singular value of $G(\mathbf{i}\omega)$, it is locally Lipschitz (e.g. [GV13, Corollary 8.6.2]). Furthermore, in the process of showing that the BBBS algorithm using the original midpoint scheme is quadratically convergent, [BB90] showed that $g_c(\omega)$ is in fact *twice differentiable at local maximizers*. The direct consequence is that Newton's method for optimization can be expected to converge quadratically when it is used to find a local maximizer of $g_c(\omega)$. Since there is only one optimization variable, namely ω , there is also the benefit that we need only work with first and second derivatives, instead of gradients and Hessians, respectively. Even without computing $g_c''(\omega)$, the secant method (which is a quasi-Newton method in one variable) would still provide superlinear convergence using only first-order information.

As long as we also compute the associated left and right singular vectors $u(\omega)$ and $v(\omega)$ when computing $g_c(\omega)$, the value of the first derivative $g_c'(\omega)$ needed by the secant method can be computed at roughly the same cost as $g_c(\omega)$, by using the direct

formulation of $g'_c(\omega)$ given in (14) (and without ever having to compute and store the eigenvectors of (4)). Furthermore, an LU factorization of $(i\omega E - A)$ can be done once and reused to solve the linear systems due to the presence of $(i\omega E - A)^{-1}$, which appears once in $g_c(\omega)$ and twice in $g'_c(\omega)$.

To compute $g''_c(\omega)$, we will need the following result for the second derivative of eigenvalues, which can be found in various forms in [Lan64], [OW95], and [Kat82].

Theorem 4.1. *For $t \in \mathbb{R}$, let $H(t)$ be a twice-differentiable $n \times n$ Hermitian matrix family with distinct eigenvalues, with the k th eigenpair denoted by $(\lambda_k(t), x_k(t))$ and ordering $\lambda_1 > \dots > \lambda_n$. Then:*

$$\lambda''_1(t) \Big|_{t=0} = x_1^* H''(0) x_1 + 2 \sum_{k=2}^n \frac{|x_1^* H'(0) x_k|^2}{\lambda_1 - \lambda_k}.$$

Since $g_c(\omega)$ is the largest singular value of $\|G(i\omega)\|_2$, it is also the largest eigenvalue of the matrix:

$$H(\omega) = \begin{bmatrix} 0 & G_c(\omega) \\ G_c(\omega)^* & 0 \end{bmatrix}, \quad (16)$$

which has first and second derivatives

$$H'(\omega) = \begin{bmatrix} 0 & G'_c(\omega) \\ G'_c(\omega)^* & 0 \end{bmatrix} \quad \text{and} \quad H''(\omega) = \begin{bmatrix} 0 & G''_c(\omega) \\ G''_c(\omega)^* & 0 \end{bmatrix}. \quad (17)$$

The formula for $G'_c(\omega)$ is given by (14) while the corresponding second derivative is obtained by straightforward application of matrix differentiation rules:

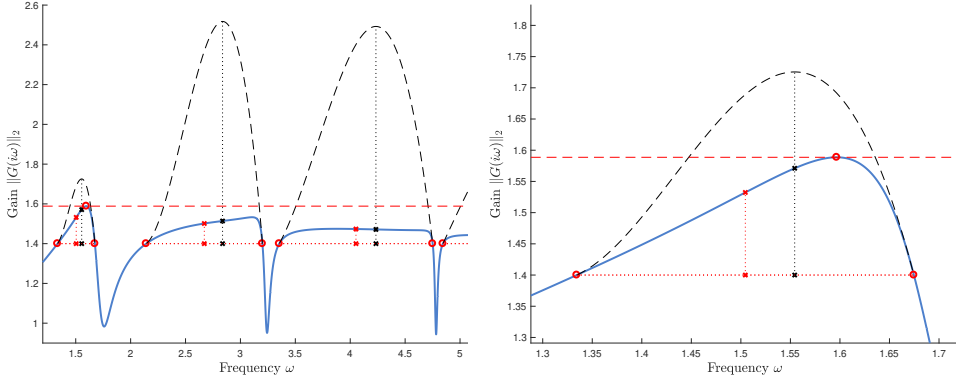
$$G''_c(\omega) = -2C(i\omega E - A)^{-1} E(i\omega E - A)^{-1} E(i\omega E - A)^{-1} B. \quad (18)$$

As an LU factorization of $(i\omega E - A)$ has already been computed and saved for reuse in order to compute $g_c(\omega)$ and $g'_c(\omega)$, computing (18) is not particularly more expensive than previous computations. However, $H(\omega)$ and its matrix derivatives in (17) are $(m+p) \times (m+p)$ matrices and the full eigenvalue decomposition of $H(\omega)$ must be computed in order to use Theorem 4.1 to compute the second derivative of the largest singular value. Thus, computing $g''_c(\omega)$ also involves $\mathcal{O}((m+p)^3)$ work in addition to the aforementioned linear solves. If $m+p \ll n$, then computing $g''_c(\omega)$ will still be relatively cheap and it would thus make sense to use Newton's method for finding local maximizers. However, as $m+p$ grows larger, at some point it will actually be faster in practice to forgo computing the second derivative and instead use the secant method, even though its slower superlinear rate of convergence will usually modestly increase the number of evaluations of $g_c(\omega)$.

Thus, our new proposed improvement to the BBBS algorithm is to not settle for the increase in γ provided by the standard midpoint or cubic interpolation schemes, but to increase γ *as far as possible* using standard optimization techniques applied to $g_c(\omega)$ at every iteration. Let

$$\hat{\omega}_j = \arg \max g_c(\omega_k) \quad \text{where} \quad \hat{\omega}_k \text{ are as defined in either (7) or (9)},$$

that is, $\hat{\omega}_j \in I_j$ is the frequency that provides the updated value γ_{mp} or γ_{cubic} in the standard algorithms. Then, depending on how $m+p$ compares to n , Newton's method



(a) Optimization-based approach

(b) Close up of leftmost peak in Figure 2a

Figure 2: For the same example as Figure 1, the larger increase in γ attained by optimizing (19) is shown by the red dashed line going through the red circle at the top of the leftmost peak of $\|G(i\omega)\|_2$. By comparison, the BBBS midpoint (red dotted vertical lines and x's) and the cubic-interpolant-based schemes (black dotted vertical lines and x's) only provide suboptimal increases in γ .

or the secant method can more or less be automatically chosen to most efficiently solve the following optimization problem with a simple box constraint:

$$\gamma_{\text{opt}} = \max_{\omega \in I_j} g_c(\omega). \quad (19)$$

Assuming the usual case that either $g'_c(\omega) > 0$ at the left endpoint of the interval I_j holds or is strictly negative at the right endpoint, and that the optimization method initial point is set to $\hat{\omega}_j$, then finding any maximizer of (19) guarantees that

$$\gamma_{\text{opt}} > \max\{\gamma_{\text{mp}}, \gamma_{\text{cubic}}\}$$

must hold, provided that $\hat{\omega}_j$ does not happen to be a stationary point of $g_c(\omega)$ with $g_c(\hat{\omega}_j)$ equal to γ_{mp} or γ_{cubic} , as appropriate. This holds true even if the optimization only finds a local maximizer of (19) on the interval. Furthermore, setting tight tolerances for the optimization code allows maximizers of (19) to be computed to full precision with little to no penalty, due to the superlinear or quadratic rate of convergence we can expect from the secant method or Newton's method, respectively. If the computed optimizer of (19) also happens to be a global maximizer of $g_c(\omega)$, for all $\omega \in \mathbb{R}$, then the \mathcal{H}_∞ norm has indeed been computed to full precision, but the algorithm must still verify this by computing the imaginary eigenvalues of $(\mathcal{M}_\gamma, \mathcal{N})$ just one more time. However, if a global optimizer hasn't yet been found, then the algorithm must compute the imaginary eigenvalues of $(\mathcal{M}_\gamma, \mathcal{N})$ at least two times more: one or more times as the algorithm increases γ to the globally optimal value, and then a final evaluation to verify that the computed value is indeed globally optimal. Figure 2 shows a pictorial comparison of optimizing $g_c(\omega)$ compared to the midpoint and cubic-interpolant-based updating methods.

We can further reduce the likelihood of incurring additional evaluations of computing the eigenvalues of $(\mathcal{M}_\gamma, \mathcal{N})$. First, computing maximizers of (19) over multiple intervals

instead of just I_j will increase the chances that a global maximizer is found at every iteration. On a single core, optimizing over too many intervals could increase the running time to the point that evaluating $g_c(\omega)$ many times could become more expensive than computing the eigenvalues of $(\mathcal{M}_\gamma, \mathcal{N})$. However, on modern hardware with multiple cores, optimizing (19) for several intervals, e.g. one per available core, is an embarrassingly parallel task and thus should not increase running times noticeably. In practice, we have found that prioritizing which intervals to optimize (when not optimizing all of them) is usually best done by first evaluating $g_c(\omega)$ at all the $\hat{\omega}_k$ values and then choosing the intervals I_k to optimize where $g_c(\hat{\omega}_k)$ takes on the largest values. Second, a global maximizer of $g_c(\omega)$ can potentially be found before ever computing eigenvalues of $(\mathcal{M}_\gamma, \mathcal{N})$ even once, by initializing the algorithm at an actual maximizer of $g_c(\omega)$ obtained via standard optimization (but now without any box constraint):

$$\gamma_{\text{init}} = \max g_c(\omega), \quad (20)$$

instead of just at some guess, which may or may not be even locally optimal. Again, we can increase the chance of computing γ_{init} equal to the actual value of the \mathcal{H}_∞ norm by optimizing (20) from multiple different starting guesses in parallel, also prioritizing the frequency guesses that most maximize $g_c(\omega)$ first.

Algorithm 2 provides a high-level pseudocode description of our improved method. We note that the initialization phase, lines 2-6, can also be used to approximate the \mathcal{H}_∞ norm of large-scale systems, provided that $(\mathbf{i}\omega E - A)^{-1}$ still permits fast linear solves.

Lastly, as a final step in the algorithm, it is necessary to check whether or not the value of the \mathcal{H}_∞ norm is attained at $\omega = \infty$. We check this case after the convergent phase has computed a global maximizer over the union of all intervals it has considered. The only possibility that the \mathcal{H}_∞ norm may be attained at $\omega = \infty$ in Algorithm 2 is when the initial value of γ computed in line 5 of is less than $\|D\|_2$. As the assumptions of Theorem 2.1 require that γ not be a singular value of D , it is not valid to use $\gamma = \|D\|_2$ in $(\mathcal{M}_\gamma, \mathcal{N})$ to check if this pencil has any imaginary eigenvalues. However, if the optimizer computed by the convergent phase of Algorithm 2 yields a γ value less than $\|D\|_2$, then it is clear that the optimizing frequency is at $\omega = \infty$.

5 Handling discrete-time systems

Now consider the discrete-time linear dynamical system

$$Ex_{k+1} = Ax_k + Bu_k \quad (21a)$$

$$y_k = Cx_k + Du_k, \quad (21b)$$

where the matrices are defined as before in (1). In this case, the \mathcal{H}_∞ norm is defined as

$$\|G\|_{\mathcal{H}_\infty} := \max_{\theta \in [0, 2\pi)} \|G(e^{i\theta})\|_2, \quad (22)$$

again assuming that pencil (A, E) is at most index one. If all finite eigenvalues are either strictly inside the unit disk centered at the origin or are uncontrollable or unobservable, then (22) is finite and the \mathcal{H}_∞ norm is attained at some $\theta \in [0, 2\pi)$. Otherwise, it is infinite.

Algorithm 2 The Improved Algorithm Using Optimization and Parallelization

Input: $A \in \mathbb{C}^{n \times n}$, $B \in \mathbb{C}^{n \times p}$, $C \in \mathbb{C}^{m \times n}$, $D \in \mathbb{C}^{m \times p}$, $E \in \mathbb{C}^{n \times n}$, initial guesses $\{\omega_1, \dots, \omega_q\} \in \mathbb{R}$ and c the number of intervals/frequencies to optimize per round.
Output: $\gamma = \|G\|_{\mathcal{H}_\infty}$ and ω such that $\gamma = g_c(\omega)$.

```

1: // Initialization:
2: Compute  $[\gamma_1, \dots, \gamma_q] = [g_c(\omega_1), \dots, g_c(\omega_q)]$ . // parallel
3: Reorder  $\{\omega_1, \dots, \omega_q\}$  s.t.  $\gamma_j \geq \gamma_{j+1}$ .
4: Compute  $[\gamma_1, \dots, \gamma_c]$  by solving (20) initialized at  $\omega_j$ ,  $j = 1, \dots, c$ . // parallel
5:  $\gamma = \max([\gamma_1, \dots, \gamma_c])$ .
6:  $\omega = \arg \max([\gamma_1, \dots, \gamma_c])$  for  $j = 1, \dots, c$ .
7: // Convergent Phase:
8: while not converged do
9:   // Compute the intervals that lie under  $g_c(\omega)$  using eigenvalues of the pencil:
10:  Compute  $\Lambda_I = \{\text{Im } \lambda : \lambda \in \Lambda(\mathcal{M}_\gamma, \mathcal{N}) \text{ and } \text{Re } \lambda = 0\}$ .
11:  Index and sort  $\Lambda_I = \{\omega_1, \dots, \omega_l\}$  s.t.  $\omega_j \leq \omega_{j+1}$ .
12:  Form all intervals  $I_k = [\omega_k, \omega_{k+1}]$  s.t.  $g'_c(\omega_k) \geq 0$  and  $g'_c(\omega_{k+1}) \leq 0$ .
13:  // Compute candidate frequencies for each interval:
14:  Compute all  $\hat{\omega}_k$  using either (7) or (9).
15:  // Run box-constrained optimization on the  $c$  most promising frequencies:
16:  Compute  $[\gamma_1, \dots, \gamma_q] = [g_c(\hat{\omega}_1), \dots, g_c(\hat{\omega}_q)]$ . // parallel
17:  Reorder  $\{\hat{\omega}_1, \dots, \hat{\omega}_q\}$  and intervals  $I_k$  s.t.  $\gamma_j \geq \gamma_{j+1}$ .
18:  Compute  $[\gamma_1, \dots, \gamma_c]$  by solving (19) initialized at  $\hat{\omega}_j$ ,  $j = 1, \dots, c$ . // parallel
19:  // Update to the highest gain computed:
20:   $\gamma = \max([\gamma_1, \dots, \gamma_c])$ .
21:   $\omega = \arg \max([\gamma_1, \dots, \gamma_c])$  for  $j = 1, \dots, c$ .
22: end while
23: // Check that the maximizing frequency isn't at infinity (continuous-time only)
24: if  $\gamma < \|D\|_2$  then
25:    $\gamma = \|D\|_2$ .
26:    $\omega = \infty$ .
27: end if

```

NOTE: The places where embarrassingly parallel processing can be used to increase the chance of finding a global optimizer of $g_c(\omega)$, without increasing the runtime given at least c cores, are marked via the comments “parallel”.

We now show the analogous version of Theorem 2.1 for discrete-time systems, which generalizes [Bye88, Theorem 4]² for the special case of simple ODEs, that is, when $B = C = E = I$ and $D = 0$. This result relates singular values of the transfer function for discrete-time systems to eigenvalues with modulus one of another associated matrix pencil. Although this discrete-time analog result is already known, the proof, to the best

²Note that equation (10) in [Bye88] has a typo: $A^H - e^{i\theta}I$ in the lower left block of $K(\theta)$ should actually be $A^H - e^{-i\theta}I$.

of our knowledge, is not in the literature so we include it in full here. The proof follows a similar argumentation as the proof of Theorem 2.1.

Theorem 5.1. *Let $\lambda E - A$ be regular with no finite eigenvalues on the unit circle, $\gamma > 0$ not a singular value of D , and $\theta \in [0, 2\pi)$. Consider the matrix pencil $(\mathcal{M}_\gamma, \mathcal{N})$, where*

$$\begin{aligned}\mathcal{M}_\gamma &:= \begin{bmatrix} A - BR^{-1}D^*C & -\gamma BR^{-1}B^* \\ 0 & E^* \end{bmatrix}, \\ \mathcal{N} &:= \begin{bmatrix} E & 0 \\ -\gamma C^*S^{-1}C & A^* - C^*DR^{-1}B^* \end{bmatrix},\end{aligned}\tag{23}$$

$R = D^*D - \gamma^2 I$ and $S = DD^* - \gamma^2 I$. Then $e^{i\theta}$ is an eigenvalue of matrix pencil $(\mathcal{M}_\gamma, \mathcal{N})$ if and only if γ is a singular value of $G(e^{i\theta})$.

Proof. Let γ be a singular value of $G(e^{i\theta})$ with left and right singular vectors u and v , that is, so that $G(e^{i\theta})v = \gamma u$ and $G(e^{i\theta})^*u = \gamma v$. Using the expanded versions of these two equivalences

$$\left(C \left(e^{i\theta} E - A \right)^{-1} B + D \right) v = \gamma u \quad \text{and} \quad \left(C \left(e^{i\theta} E - A \right)^{-1} B + D \right)^* u = \gamma v, \tag{24}$$

we define

$$q = \left(e^{i\theta} E - A \right)^{-1} B v \quad \text{and} \quad s = \left(e^{-i\theta} E^* - A^* \right)^{-1} C^* u. \tag{25}$$

Rewriting (24) using (25) yields the following matrix equation:

$$\begin{bmatrix} C & 0 \\ 0 & B^* \end{bmatrix} \begin{bmatrix} q \\ s \end{bmatrix} = \begin{bmatrix} -D & \gamma I \\ \gamma I & -D^* \end{bmatrix} \begin{bmatrix} v \\ u \end{bmatrix} \implies \begin{bmatrix} v \\ u \end{bmatrix} = \begin{bmatrix} -D & \gamma I \\ \gamma I & -D^* \end{bmatrix}^{-1} \begin{bmatrix} C & 0 \\ 0 & B^* \end{bmatrix} \begin{bmatrix} q \\ s \end{bmatrix}, \tag{26}$$

where

$$\begin{bmatrix} -D & \gamma I \\ \gamma I & -D^* \end{bmatrix}^{-1} = \begin{bmatrix} -R^{-1}D^* & -\gamma R^{-1} \\ -\gamma S^{-1} & -DR^{-1} \end{bmatrix} \quad \text{and} \quad \begin{bmatrix} q \\ s \end{bmatrix} \neq 0. \tag{27}$$

Rewriting (25) as:

$$\left(\begin{bmatrix} e^{i\theta} E & 0 \\ 0 & e^{-i\theta} E^* \end{bmatrix} - \begin{bmatrix} A & 0 \\ 0 & A^* \end{bmatrix} \right) \begin{bmatrix} q \\ s \end{bmatrix} = \begin{bmatrix} B & 0 \\ 0 & C^* \end{bmatrix} \begin{bmatrix} v \\ u \end{bmatrix}, \tag{28}$$

and then substituting in (26) for the rightmost term of (28) yields

$$\left(\begin{bmatrix} e^{i\theta} E & 0 \\ 0 & e^{-i\theta} E^* \end{bmatrix} - \begin{bmatrix} A & 0 \\ 0 & A^* \end{bmatrix} \right) \begin{bmatrix} q \\ s \end{bmatrix} = \begin{bmatrix} B & 0 \\ 0 & C^* \end{bmatrix} \begin{bmatrix} -D & \gamma I \\ \gamma I & -D^* \end{bmatrix}^{-1} \begin{bmatrix} C & 0 \\ 0 & B^* \end{bmatrix} \begin{bmatrix} q \\ s \end{bmatrix}. \tag{29}$$

Multiplying the above on the left by

$$\begin{bmatrix} I & 0 \\ 0 & -e^{i\theta} I \end{bmatrix}$$

and then rearranging terms, we have

$$e^{i\theta} \begin{bmatrix} E & 0 \\ 0 & A^* \end{bmatrix} \begin{bmatrix} q \\ s \end{bmatrix} = \begin{bmatrix} A & 0 \\ 0 & E^* \end{bmatrix} \begin{bmatrix} q \\ s \end{bmatrix} + \begin{bmatrix} B & 0 \\ 0 & -e^{i\theta} C^* \end{bmatrix} \begin{bmatrix} -D & \gamma I \\ \gamma I & -D^* \end{bmatrix}^{-1} \begin{bmatrix} C & 0 \\ 0 & B^* \end{bmatrix} \begin{bmatrix} q \\ s \end{bmatrix}.$$

Substituting the inverse in (27) for its explicit form and multiplying terms yields:

$$e^{i\theta} \begin{bmatrix} E & 0 \\ 0 & A^* \end{bmatrix} \begin{bmatrix} q \\ s \end{bmatrix} = \begin{bmatrix} A & 0 \\ 0 & E^* \end{bmatrix} \begin{bmatrix} q \\ s \end{bmatrix} + \begin{bmatrix} B & 0 \\ 0 & -e^{i\theta} C^* \end{bmatrix} \begin{bmatrix} -R^{-1} D^* C & -\gamma R^{-1} B^* \\ -\gamma S^{-1} C & -D R^{-1} B^* \end{bmatrix} \begin{bmatrix} q \\ s \end{bmatrix}.$$

Finally, multiplying terms further, separating out the $-e^{i\theta}$ terms to bring them over to the left hand side, and then recombining, we have that

$$e^{i\theta} \begin{bmatrix} E & 0 \\ -\gamma C^* S^{-1} C & A^* - C^* D R^{-1} B^* \end{bmatrix} \begin{bmatrix} q \\ s \end{bmatrix} = \begin{bmatrix} A - B D R^{-1} B^* & -\gamma B R^{-1} B^* \\ 0 & E^* \end{bmatrix} \begin{bmatrix} q \\ s \end{bmatrix}.$$

It is now clear that $e^{i\theta}$ is an eigenvalue of pencil $(\mathcal{M}_\gamma, \mathcal{N})$.

Now suppose that $e^{i\theta}$ is an eigenvalue of pencil $(\mathcal{M}_\gamma, \mathcal{N})$ with eigenvector given by q and s as above. Then it follows that (29) holds, which can be rewritten as (28) by defining u and v using the right-hand side equation of (26), noting that neither can be identically zero. It is then clear that the pair of equivalences in (25) hold. Finally, substituting (25) into the left-hand side equation of (26), it is clear that γ is a singular value of $G(e^{i\theta})$, with left and right singular vectors u and v . \square

Adapting Algorithm 2 to the discrete-time case is straightforward. First, all instances of $g_c(\omega)$ must be replaced with

$$g_d(\theta) := \|G(e^{i\theta})\|_2.$$

To calculate its first and second derivatives, we will need the first and second derivatives of $G_d(\theta) := G(e^{i\theta})$ and for notational brevity, it will be convenient to define $Z(\theta) := (e^{i\theta} E - A)$. Then

$$G'_d(\theta) = -\operatorname{Re} \left(i e^{i\theta} C Z(\theta)^{-1} E Z(\theta)^{-1} B \right) \quad (30)$$

and

$$G''_d(\theta) = \operatorname{Re} \left(e^{i\theta} C Z(\theta)^{-1} E Z(\theta)^{-1} B \right) - 2 \operatorname{Re} \left(e^{2i\theta} C Z(\theta)^{-1} E Z(\theta)^{-1} E Z(\theta)^{-1} B \right). \quad (31)$$

The first derivative of $g_d(\theta)$ can thus be calculated using (13), where ω , $g_c(\omega)$, and $G'_c(\omega)$ are replaced by θ , $g_d(\theta)$, and $G'_d(\theta)$ using (30). The second derivative of $g_d(\theta)$ can be calculated using Theorem 4.1 using (30) and (31) to define $H(\theta)$, the analog of (16). Line 10 must be changed to instead compute the eigenvalues of unit modulus of (23). Line 11 must instead index and sort the angles $\{\theta_1, \dots, \theta_l\}$ of these unit modulus eigenvalues in ascending order. Due to the periodic nature of (22), line 12 must additionally consider the interval $[\theta_l, \theta_0 + 2\pi]$.

6 Numerical experiments

We implemented Algorithm 2 in MATLAB, for both continuous-time and discrete-time cases. Since we can only get timing information from `hinfnorm` and we wished to verify that our new method does indeed reduce the number of times the eigenvalues of $(\mathcal{M}_\gamma, \mathcal{N})$ are computed, we also designed our code so that it can run just using the

standard BBBS algorithm or the cubic-interpolant scheme. For our new optimization-based approach, we used `fmincon` for both the unconstrained optimization calls needed for the initialization phase and for the box-constrained optimization calls needed in the convergent phase; `fmincon`'s optimality and constraint tolerances were set to 10^{-14} in order to find maximizers to near machine precision. Our code supports starting the latter optimization calls from either the midpoints of the BBBS algorithm (7) or the maximizing frequencies calculated from the cubic-interpolant method (9). Furthermore, the optimizations may be done using either the secant method (first-order information only) or with Newton's method using second derivatives, thus leading to four variants of our proposed method to test. Our code has a user-settable parameter that determines when $m + p$ should be considered too large relative to n , and thus when it is likely that using secant method will actually be faster than Newton's method, due to the additional expense of computing the second derivative of the norm of the transfer function.

Though our algorithm affords many opportunities for parallelization, we found that the overhead cost when using the MATLAB directive `parfor` often negated any speedup advantages. As such, we tested our code with serial computation only, that is, we only optimized one interval/frequency per round ($c = 1$ in Algorithm 2). We expect that an implementation in Fortan or C would demonstrate the benefits of optimizing $g_c(\omega)$ over multiple intervals and from multiple starting frequencies in parallel.

For initial frequency guesses, our code simply tests zero and the imaginary part of the rightmost eigenvalue of (A, E) , excluding eigenvalues that are either infinite, uncontrollable, or unobservable. Eigenvalues are deemed uncontrollable or unobservable if $\|B^*y\|_2$ or $\|Cx\|_2$ are respectively below a user-set tolerance, where x and y are respectively the right and left eigenvectors for a given eigenvalue of (A, E) . In the discrete-time case, the default initial guesses are zero, π , and the angle for the largest modulus eigenvalue.³

For efficiency of implementing our method and conducting these experiments, our code does not yet take advantage of structure-preserving eigensolvers. Instead, it uses the regular QZ algorithm (`eig` in MATLAB) to compute the eigenvalues of $(\mathcal{M}_\gamma, \mathcal{N})$. To help mitigate issues due to rounding errors, we keep any computed eigenvalue λ if $|\operatorname{Re} \lambda| \leq \tau_\lambda$ with $\tau_\lambda = 10^{-8}$ as a potentially purely imaginary eigenvalue. Taking the real parts of these nearly imaginary eigenvalues forms the initial set of candidate frequencies (or nearly unit modulus eigenvalues and their angles for the discrete-time case). Then, we evaluate $\|G(\mathbf{i}\omega)\|_2$ at these candidate frequencies (or $\|G(e^{i\theta})\|_2$ at the candidate angles) and only keep the frequencies (angles) for eigenvalues λ where $\|G(\mathbf{i}\operatorname{Re} \lambda)\|_2$ ($\|G(e^{i\angle \lambda})\|_2$) agrees to the current value of γ to at least two digits. Note that while this strategy is sufficient for our experimental comparisons here, it is certainly not always reliable in practice. For example, the correct frequencies will not be calculated for the challenging `peec` test problem from the SLICOT benchmark examples⁴, unless τ_λ is increased to 10^{-5} (but then this work-around strategy is quite expensive as there are many computed eigenvalues near the imaginary axis that must be evaluated for this problem).

All experiments were performed using MATLAB R2016b running on a Macbook Pro

³ For producing a production-quality implementation, see [BS90] for more sophisticated initial guesses that can be used, [BV11, Section III] for dealing with testing properness of the transfer function, and [Var90] for filtering out uncontrollable/unobservable eigenvalues of (A, E) when it has index higher than one.

⁴ Available at <http://slicot.org/20-site/126-benchmark-examples-for-model-reduction>

with an Intel i7-6567U dual-core CPU, 16GB of RAM, and Mac OS X v10.12.

6.1 \mathcal{H}_∞ computation experiments (small scale)

We evaluated our code on several continuos-time problems up to moderate dimensions taken from the test set used in [GGO13] (problems CBM, CSE2, CM3, CM4, NN18) and the SLICOT benchmark examples (problems ISS and FOM), as well as two new randomly-generated examples (using `randn()`) with a relatively large number of inputs and outputs. See Table 1 for the exact dimensions of these problems. On all examples, the \mathcal{H}_∞ norm values computed by our code (in all its variants) agreed to at least 12 digits with the results provided by `hinfnorm` also used with a tight tolerance of 10^{-14} ; usually our code found slightly larger values, i.e., more accurate values since our method optimizes $g_c(\omega)$ directly.

In Table 3, we list the number of times the eigenvalues $(\mathcal{M}_\gamma, \mathcal{N})$ were computed and the number of evaluations of $g_c(\omega)$ for our new method compared to the existing BBBS algorithm and its interpolation-based refinement. As can be seen, our new method typically limits the number of required eigenvalue computations of $(\mathcal{M}_\gamma, \mathcal{N})$ to just two, and often it only requires one (in the cases where our method found a global optimizer of $g_c(\omega)$ in the initialization phase). In contrast, the standard BBBS algorithm and its interpolation-based refinement must evaluate the eigenvalues $(\mathcal{M}_\gamma, \mathcal{N})$ more times; for example, on problem CBM, the BBBS algorithm needed eight evaluations while its interpolation-based refinement still needed five. While our new method often requires more evaluations of $g_c(\omega)$ than the previous methods, the increase is generally not substantial. We also observe that employing the secant method in lieu of Newton's method generally results in more evaluations of $g_c(\omega)$, though the difference is not dramatic, as we'd expect.

In Table 4, we compare the corresponding wall-clock times, and for convenience, we replicate the timing results of `hinfnorm` from Table 1 on the same problems. We observe that our new method is fastest on seven out of the nine test problems, often significantly so. Compared to our own implementation of the BBBS algorithm, our new method is on average twice as fast and sometimes up to three times faster. Our method is even faster when compared to `hinfnorm`, which has the advantage of being a compiled code rather than interpreted like our code. Our new method is over 12 times faster than `hinfnorm` overall, but this is largely due to the three problems (FOM, NN18, and `randn 1`) where our code is 25-35 times faster. We suspect that this large performance gap on these problems is not necessarily due to a correspondingly dramatic reduction in the number of times that the eigenvalues of $(\mathcal{M}_\gamma, \mathcal{N})$ are computed but rather that the structure-preserving eigensolver `hinfnorm` employs sometimes has a steep performance penalty compared to standard QZ. However, it is difficult to verify this as `hinfnorm` is not open source. We also see that for the variants of our method, there is about a 25% percent penalty on average in the runtime when resorting to the secant method instead of Newton's method. The notable exception is problem `randn 1` where using the secant method is slightly faster than using Newton, but this is also as expected since for this problem, $m + p$ is actually larger than n ($m = p = 300$ and $n = 500$). Nonetheless, even the slower secant-method-based version of our hybrid optimization approach is still typically much faster than BBBS or the cubic-interpolation scheme.

Problem	Hybrid Optimization				Standard Algs.	
	Newton		Secant			
	Interp.	MP	Interp.	MP	Interp.	BBBS
Number of Eigenvalue Computations of $(\mathcal{M}_\gamma, \mathcal{N})$						
CBM	2	2	2	2	5	8
CSE2	2	2	1	1	2	3
CM3	2	3	2	2	3	4
CM4	2	2	2	2	4	6
ISS	1	1	1	1	3	4
FOM	1	1	1	1	2	2
NN18	1	1	1	1	2	2
randn 1	1	1	1	1	1	1
randn 2	1	1	1	1	2	2
Number of Evaluations of $g_c(\omega)$						
CBM	41	40	67	67	64	93
CSE2	15	9	10	10	13	19
CM3	48	53	70	71	47	52
CM4	22	23	46	46	73	88
ISS	12	12	22	22	58	63
FOM	4	4	16	16	7	7
NN18	4	4	8	8	7	7
randn 1	1	1	1	1	1	1
randn 2	4	4	17	17	7	7

Table 3: The top half of the table reports the number of times the eigenvalues of $(\mathcal{M}_\gamma, \mathcal{N})$ were computed in order to compute the \mathcal{H}_∞ norm to near machine precision. From left to right, the methods are our hybrid optimization approach using Newton’s method and the secant method, the cubic-interpolant scheme (column ‘Interp.’) and the standard BBBS method, all implemented by our single configurable code. The subcolumns ‘Interp.’ and ‘MP’ of our methods respectively indicate that the optimization routines were initialized at the points from the cubic-interpolant scheme and the BBBS midpoint scheme. The bottom half of the table reports the number of times it was necessary to evaluate the norm of the transfer function (with or without its derivatives).

On the two problems (CSE2 and CM3) where our new method is not fastest, the small dimensions are likely a significant factor, since the performance gap between computing $g_c(\omega)$ and the eigenvalues $(\mathcal{M}_\gamma, \mathcal{N})$ becomes smaller as n decreases. Indeed, CSE2 and CM3 are the smallest examples in our test sets, respectively $n = 63$ and $n = 123$. However, our method did compute the eigenvalues of $(\mathcal{M}_\gamma, \mathcal{N})$ less times than the existing methods for these two problems, as desired, and the corresponding increase in the number of evaluations of $g_c(\omega)$ was only moderate for CM3 and actually decreased for CSE2. As such, we suspect that our code being implemented in an interpreted language and having not yet been optimized also impacted performance.

Problem	Hybrid Optimization				Standard Algs.		<code>hinfnorm(·, tol)</code>	
	Newton		Secant				tol	
	Interp.	MP	Interp.	MP	Interp.	BBBS	1e-14	0.01
Wall-clock running times in seconds								
CBM	1.020	0.979	1.548	1.824	1.948	3.102	3.050	2.928
CSE2	0.054	0.052	0.044	0.040	0.031	0.043	0.131	0.093
CM3	0.177	0.226	0.314	0.322	0.230	0.252	0.142	0.055
CM4	0.413	0.402	0.606	0.655	1.091	1.302	1.514	0.708
ISS	0.437	0.415	0.409	0.397	1.126	1.271	0.713	0.455
FOM	2.922	2.931	3.892	3.902	6.026	5.846	100.774	35.384
NN18	2.896	2.912	3.928	3.295	6.230	6.253	100.783	35.798
randn 1	0.835	0.790	0.723	0.754	0.761	0.734	21.079	24.209
randn 2	7.797	7.825	8.570	8.473	17.014	15.148	27.315	15.698
Running times relative to hybrid optimization (Newton with ‘Interp.’)								
CBM	1	0.96	1.52	1.79	1.91	3.04	2.99	2.87
CSE2	1	0.97	0.80	0.74	0.56	0.79	2.41	1.72
CM3	1	1.28	1.77	1.82	1.30	1.43	0.80	0.31
CM4	1	0.97	1.47	1.59	2.64	3.15	3.66	1.71
ISS	1	0.95	0.93	0.91	2.57	2.91	1.63	1.04
FOM	1	1.00	1.33	1.34	2.06	2.00	34.48	12.11
NN18	1	1.01	1.36	1.14	2.15	2.16	34.80	12.36
randn 1	1	0.95	0.86	0.90	0.91	0.88	25.23	28.98
randn 2	1	1.00	1.10	1.09	2.18	1.94	3.50	2.01
Average	1	1.01	1.24	1.26	1.81	2.03	12.17	7.01

Table 4: In the top half of the table, the running times (fastest in bold) are reported for the same methods and configurations as in Table 3, with the running times of `hinfnorm` additionally listed in the rightmost two columns, for a tolerance of 10^{-14} (as used by the other methods) and its default value of 0.01. The bottom half of the table normalizes all the times relative to the running times for our hybrid optimization method (Newton and ‘Interp.’), along with the overall averages relative to this variant.

6.2 \mathcal{H}_∞ approximation experiments (large scale)

As mentioned towards the end of Section 4, the initialization phase of Algorithm 2 also provides a scalable approach to approximating the \mathcal{H}_∞ norm, though the sparse version of the code should still return the value of $\|D\|_2$ as the \mathcal{H}_∞ norm approximation if the optimal value of γ computed in line 5 is not as large. Table 5 shows our selection of large-scale test problems; problems `dwave` and `markov` are from the large-scale test set used in [GGO13] while the remaining problems are freely available from the website of Joost Rommes⁵. As $m + p \ll n$ holds in all of these examples, we just present results for our code when using Newton’s method.

⁵Available at <https://sites.google.com/site/rommes/software>

Large-scale test problems				
Problem	n	p	m	$E = I$
<code>dwave</code>	2048	4	6	Y
<code>markov</code>	5050	4	6	Y
<code>bips98_1450</code>	11305	4	4	N
<code>bips07_1693</code>	13275	4	4	N
<code>bips07_1998</code>	15066	4	4	N
<code>bips07_2476</code>	16861	4	4	N
<code>descriptor_xingo6u</code>	20738	1	6	N
<code>mimo8x8_system</code>	13309	8	8	N
<code>mimo28x28_system</code>	13251	28	28	N
<code>ww_vref_6405</code>	13251	1	1	N
<code>xingo_afonso_itaipu</code>	13250	1	1	N

Table 5

Since directly optimizing $g_c(\omega)$ involves solving linear systems for $(i\omega E - A)^{-1}$, we compare our approach with one of the \mathcal{H}_∞ norm approximation methods that also requires solving linear systems, namely the MATLAB code `hinorm`, which implements the spectral-value-set-based method using dominant poles of [BV14]. In order to compute dominant poles at each iteration, `hinorm` uses `samdp`, which is a MATLAB code that implements the subspace-accelerated dominant pole algorithm of [RM06]. We tested `hinorm` using its default settings, noting that it initially computes 20 dominant poles to find a starting point. To similarly initialize our method, our code called `samdp` once to also compute 20 dominant poles and used their imaginary parts as starting frequencies for optimizing. We tested our method by optimizing the c most promising frequencies for $c = 1, 5, 10$ (again using serial computation, since our parallel implementation in MATLAB is not yet performant). Since we used LU decompositions to solve the linear systems, we tested our code in two configurations: using UMFPACK and using LAPACK (both provided via the MATLAB function `lu`). For all problems, our code produced \mathcal{H}_∞ norm approximations that agreed to at least 12 digits with `hinorm`, meaning that the additional optimization calls done with $c = 5$ and $c = 10$ did not produce better maximizers than what was found with $c = 1$ and thus, only added to the serial computation running time.

In Table 6, we present the running times of the codes and configurations. First, we observe that for our direct optimization method, using the UMFPACK code path of `lu` is two to eight times faster than when it is configured to use the LAPACK code path; on average, using UMFPACK is typically 2.5 times faster. Interestingly, on the last five problems, using `lu`'s LAPACK code path was actually best, but the UMFPACK variant was typically only about 25% slower and at worse, about 1.7 times slower (`descriptor_xingo6u`). We found that our direct optimization approach, using just one starting frequency ($c = 1$) was typically 3.7 times faster than `hinorm` on average and almost up to 10 times faster on problem `bips07_1693`. Only on problem `dwave` was our method actually slower than `hinorm` and only by a negligible amount. Interestingly,

Problem	Direct optimization: $c = 1, 5, 10$						hinorm	
	UMFPACK LU			LAPACK LU				
	1	5	10	1	5	10		
Wall-clock running times in seconds (initialized via <code>samdp</code>)								
dwave	1.979	1.981	1.997	5.536	5.154	5.543	1.861	
markov	3.499	3.615	3.593	26.734	26.898	27.219	3.703	
bips98_1450	6.914	8.333	10.005	14.559	17.157	19.876	31.087	
bips07_1693	8.051	9.155	11.594	18.351	21.367	24.322	75.413	
bips07_1998	10.344	11.669	13.881	50.059	56.097	59.972	51.497	
bips07_2476	14.944	16.717	18.942	65.227	70.920	73.206	76.697	
descriptor_xingo6u	13.716	15.328	16.997	7.907	9.225	11.133	36.775	
mimo8x8_system	7.566	8.934	11.211	6.162	7.562	9.321	30.110	
mimo28x28_system	12.606	17.767	20.488	10.815	16.591	21.645	33.107	
ww_vref_6405	7.353	6.785	7.552	4.542	5.076	5.437	18.553	
xingo_afonso_itaipu	5.780	6.048	7.772	4.676	4.975	5.573	16.928	
Running times relative to direct optimization (UMFPACK with $c = 1$)								
dwave	1	1.00	1.01	2.80	2.60	2.80	0.94	
markov	1	1.03	1.03	7.64	7.69	7.78	1.06	
bips98_1450	1	1.21	1.45	2.11	2.48	2.87	4.50	
bips07_1693	1	1.14	1.44	2.28	2.65	3.02	9.37	
bips07_1998	1	1.13	1.34	4.84	5.42	5.80	4.98	
bips07_2476	1	1.12	1.27	4.36	4.75	4.90	5.13	
descriptor_xingo6u	1	1.12	1.24	0.58	0.67	0.81	2.68	
mimo8x8_system	1	1.18	1.48	0.81	1.00	1.23	3.98	
mimo28x28_system	1	1.41	1.63	0.86	1.32	1.72	2.63	
ww_vref_6405	1	0.92	1.03	0.62	0.69	0.74	2.52	
xingo_afonso_itaipu	1	1.05	1.34	0.81	0.86	0.96	2.93	
Average	1	1.12	1.30	2.52	2.74	2.97	3.70	

Table 6: In the top half of the table, the running times (fastest in bold) are reported for our direct Newton-method-based optimization approach in two configurations (1u using UMFPACK and 1u using LAPACK) and **hinorm**. Each configuration of our approach optimizes the norm of the transfer function for up to c different starting frequencies ($c = 1, 5, 10$), done sequentially. The bottom of half the table normalizes all the times relative to the running times for our optimization method using UMFPACK with $c = 1$, along with the overall averages relative to this variant.

optimizing just one initial frequency versus running optimization for ten frequencies ($c = 10$) typically only increased the total running time of our code by 20-30%. This strongly suggested that the dominant cost of running our method is actually just calling `samdp` to compute the 20 initial dominant poles to obtain starting guesses. As such, in Table 7, we report the percentage of the overall running time for each method that was due to their initial calls to `samdp`. Indeed, our method’s single call to `samdp` accounted

Percentage of time just to compute 20 initial dominant poles (first call to `samdp`)

Problem	Direct optimization: $c = 1, 5, 10$						<code>hinorm</code>	
	UMFPACK LU			LAPACK LU				
	1	5	10	1	5	10		
<code>dwave</code>	99.3	99.3	99.2	99.3	99.6	99.6	98.0	
<code>markov</code>	99.2	99.1	99.1	99.6	99.6	99.6	98.1	
<code>bips98_1450</code>	84.1	72.7	60.4	84.9	73.0	61.8	21.7	
<code>bips07_1693</code>	84.2	75.1	61.6	85.6	77.1	64.4	10.1	
<code>bips07_1998</code>	85.2	77.1	66.0	88.5	81.5	72.8	18.3	
<code>bips07_2476</code>	88.0	80.2	71.4	89.2	83.6	73.0	18.6	
<code>descriptor_xingo6u</code>	90.2	82.8	75.0	89.3	79.9	66.8	38.4	
<code>mimo8x8_system</code>	84.6	74.4	59.1	84.1	67.7	55.0	24.2	
<code>mimo28x28_system</code>	81.5	59.4	51.2	75.5	46.9	39.1	40.9	
<code>ww_vref_6405</code>	95.1	79.6	63.9	91.9	78.3	75.1	33.7	
<code>xingo_afonso_itaipu</code>	90.2	84.4	76.8	89.3	83.7	74.7	33.6	

Table 7: The column headings are the same as in Table 6.

for 81.5-99.3% of its running-time (using UMFPACK with $c = 1$). In contrast, `hinorm`'s initial call to `samdp` usually accounted for about only a quarter of its running time on average, excluding `dwave` and `markov` as exceptional cases. In other words, the convergent phase of our method is actually even faster than the convergent phase of `hinorm` than what Table 6 appears to indicate. On problem `bips07_1693`, we see that our proposed method of using Newton's method to optimize $g_c(\omega)$ directly is actually over 53 times faster than `hinorm`'s convergent phase.

7 Conclusion and outlook

We have presented an improved algorithm that significantly reduces the time necessary to compute the \mathcal{H}_∞ norm of linear control systems compared to existing algorithms. Furthermore, our proposed hybrid optimization approach also allows the \mathcal{H}_∞ norm to be computed to machine precision with relatively little extra work, unlike earlier methods. Lastly, we have shown that approximating the \mathcal{H}_∞ norm of large-scale problems via directly optimizing the norm of the transfer functions is not only viable but can also be quite efficient.

The sometimes excessively longer compute times for `hinfnorm` compared to all other methods we evaluated possibly indicates that the structured-preserving eigensolver that it uses can sometimes be much slower than QZ. This certainly warrants further investigation, and if confirmed, suggests that optimizing the code/algorithm of the structured-preserving eigensolver could be a worthwhile pursuit. In the large-scale setting, we have observed that the dominant cost for our direct optimization approach is actually due to obtaining the starting frequency guesses via computing dominant poles. If the process of obtaining good initial guesses can be accelerated, then approximating the \mathcal{H}_∞ norm

via direct optimization could be significantly sped up even more.

References

- [ABM⁺16] N. Aliyev, P. Benner, E. Mengi, P. Schwerdtner, and M. Voigt. Large-scale computation of \mathcal{L}_∞ -norms by a greedy subspace method. Technical report, 2016. Submitted. Preprint available from <http://arxiv.org/abs/1705.10086>.
- [Ant05] A. C. Antoulas. *Approximation of Large-Scale Dynamical Systems*, volume 6 of *Advances in Design and Control*. SIAM Publications, Philadelphia, PA, 2005.
- [BB90] S. Boyd and V. Balakrishnan. A regularity result for the singular values of a transfer matrix and a quadratically convergent algorithm for computing its L_∞ -norm. *Syst. Cont. Lett.*, 15:1–7, 1990.
- [BBK89] S. Boyd, V. Balakrishnan, and P. Kabamba. A bisection method for computing the \mathcal{H}_∞ norm of a transfer matrix and related problems. *Math. Control Signals Systems*, 2:207–219, 1989.
- [BBMX02] P. Benner, R. Byers, V. Mehrmann, and H. Xu. Numerical computation of deflating subspaces of skew-Hamiltonian/Hamiltonian pencils. *SIAM J. Matrix Anal. Appl.*, 24(1):165–190, 2002.
- [BCOW17] P. Benner, A. Cohen, M. Ohlberger, and K. Willcox. *Model Reduction and Approximation: Theory and Algorithms*. SIAM Publications, Philadelphia, PA, 2017. ISBN: 978-1-611974-81-2.
- [BHLO06] J. V. Burke, D. Henrion, A. S. Lewis, and M. L. Overton. HIFOO - a MATLAB package for fixed-order controller design and H_∞ optimization. In *Fifth IFAC Symposium on Robust Control Design, Toulouse*, 2006.
- [BP11] M. N. Belur and C. Praagman. An efficient algorithm for computing the H_∞ norm. *IEEE Trans. Automat. Control*, 56(7):1656–1660, 2011.
- [BS90] N. A. Bruinsma and M. Steinbuch. A fast algorithm to compute the H_∞ -norm of a transfer function matrix. *Syst. Cont. Lett.*, 14(4):287–293, 1990.
- [BSV12] P. Benner, V. Sima, and M. Voigt. \mathcal{L}_∞ -norm computation for continuous-time descriptor systems using structured matrix pencils. *IEEE Trans. Automat. Control*, 57(1):233–238, 2012.
- [BSV16] P. Benner, V. Sima, and M. Voigt. Algorithm 961: Fortran 77 subroutines for the solution of skew-Hamiltonian/Hamiltonian eigenproblems. *ACM Trans. Math. Software*, 42(3):Art. 24, 26, 2016.
- [BV11] P. Benner and M. Voigt. On the computation of particular eigenvectors of Hamiltonian matrix pencils. *Proc. Appl. Math. Mech.*, 11(1):753–754, 2011.

[BV14] P. Benner and M. Voigt. A structured pseudospectral method for \mathcal{H}_∞ -norm computation of large-scale descriptor systems. *Math. Control Signals Systems*, 26(2):303–338, 2014.

[Bye88] R. Byers. A bisection method for measuring the distance of a stable to unstable matrices. *SIAM J. Sci. Statist. Comput.*, 9:875–881, 1988.

[FSV14] M. A. Freitag, A. Spence, and P. Van Dooren. Calculating the H_∞ -norm using the implicit determinant method. *SIAM J. Matrix Anal. Appl.*, 35(2):619–635, 2014.

[GGO13] N. Guglielmi, M. Gürbüzbalaban, and M. L. Overton. Fast approximation of the H_∞ norm via optimization over spectral value sets. *SIAM J. Matrix Anal. Appl.*, 34(2):709–737, 2013.

[GV13] G. H. Golub and C. F. Van Loan. *Matrix Computations*. Johns Hopkins University Press, Baltimore, fourth edition, 2013.

[GVV98] Y. Genin, P. Van Dooren, and V. Vermaut. Convergence of the calculation of \mathcal{H}_∞ -norms and related questions. In *Proceedings MTNS-98*, pages 429–432, Jul. 1998.

[Kat82] T. Kato. *A short introduction to perturbation theory for linear operators*. Springer-Verlag, New York-Berlin, 1982.

[Lan64] P. Lancaster. On eigenvalues of matrices dependent on a parameter. *Numer. Math.*, 6:377–387, 1964.

[MO16] T. Mitchell and M. L. Overton. Hybrid expansion-contraction: a robust scaleable method for approximating the H_∞ norm. *IMA J. Numer. Anal.*, 36(3):985–1014, 2016.

[OW95] M. L. Overton and R. S. Womersley. Second derivatives for optimizing eigenvalues of symmetric matrices. *SIAM J. Matrix Anal. Appl.*, 16(3):697–718, 1995.

[RM06] J. Rommes and N. Martins. Computing transfer function dominant poles of large-scale second-order dynamical systems. *IEEE Trans. Power Systems*, 21(4):1471–1483, November 2006.

[SVT95] J. Sreedhar, P. Van Dooren, and A. Tits. A fast algorithm to compute the real structured stability radius. In *Proc. Conf. Centennial Hurwitz on Stability Theory, Ticino (CH), May 21-26*, 1995.

[Var90] A. Varga. Computation of irreducible generalized state-space realizations. *Kybernetika (Prague)*, 26(2):89–106, 1990.